J Appl Electrochem (2010) 40:1991–1995
DOI 10.1007/s10800-010-0178-7

ORIGINAL PAPER

Synthesis of face centered cubic and hexagonal closed packed nickel using ionic liquids

Abhishek Lahiri · Rupak Das

Received: 5 January 2010 / Accepted: 18 July 2010 / Published online: 30 July 2010

Abstract Nickel was electrodeposited from $NiCl_2$-1-ethyl-3-methylimidazolium chloride at various temperatures at a constant potential. It was observed that by varying the electrolysis temperature, face centered cubic (FCC) and hexagonal close packed structured (HCP) nickel could be produced. From spectroscopic studies, it could be said that H^+ ions played an important role in the formation of HCP nickel. The hydrogen content in HCP nickel was found to be 1.2 wt%. From the Chronoamperometric studies, the diffusion coefficient of the electroactive species for the electrodeposition of nickel at 150 °C was estimated to be 1.1×10^{-5} cm^2 s^{-1}.

Keywords Nickel · Hydrogen storage · Electrodeposition · Ionic liquids · Diffusion coefficient

1 Introduction

Nickel has two crystal structures namely, the stable face centered cubic (FCC) and hexagonal close packed (HCP). However, the HCP nickel is considered to be metastable phase [1, 2]. The nickel hydrogen phase diagram shows that at high pressures of greater than 100 Mpa there is considerable solubility of hydrogen [3, 4]. At extremely high pressure of 1600–1900 Mpa, nickel forms a low hydrogen content α-Ni solid solution and a hydrogen rich nonstoichiometric β-Ni hydride phase [3]. Such high hydrogen fugacity can be achieved by electrochemical deposition.

FCC nickel is usually formed by reducing nickel oxide by hydrogen at high temperature [5]. On contrary, the formation of HCP nickel involves complicated steps. There are few literatures available on the synthesis of HCP nickel. Carturan et al. [6] synthesized HCP nickel by reacting Ni(II) complexes with K/B liquid alloy at 200 °C whereas Mi et al. [7] used $NiCl_2$ and reacted it with KBH_4 and ethelenediamine at temperatures ranging from 200 to 400 °C. It was also shown that HCP nickel can be obtained by sputtering nickel in hydrogen atmosphere [8]. However, pure HCP nickel phase could not be achieved by the sputtering technique.

As HCP nickel is metastable and can be formed in presence of hydrogen, we electrochemically synthesized HCP nickel from $NiCl_2$-1-ethyl-3-methylimidazolium chloride. It was observed that FCC nickel formed at 140 °C whereas HCP nickel could be formed at 160 °C.

To understand the reaction mechanism for the electrodeposition of nickel, the electrolyte was analyzed using Fourier Transform Infrared Spectroscopy (FTIR). Electrochemical studies were also performed using chronoamperometric technique. To identify the phases formed at the cathode, the material was characterized using scanning electron microscopy (SEM), Energy dispersive X-ray (EDX) and X-ray diffraction (XRD) technique.

2 Experimental

Ionic liquid of 1-ethyl-3-methylimidazolium chloride titanium metal and $NiCl_2$ were obtained from Sigma-Aldrich. 5.4 mol% of $NiCl_2$ was dissolved into EmimCl in a Pyrex

A. Lahiri · R. Das
Department of Metallurgy and Materials Engineering, University of Alabama, Tuscaloosa, AL 35487, USA

A. Lahiri (✉)
WPI AIMR, Tohoku University, Sendai 980-8579, Japan
e-mail: lahiri.abhishek@gmail.com

beaker. The experiment was conducted in a Labconco glove box filled with argon. The mixture was stirred continuously for complete dissolution. The end product obtained was liquid having green color.

Bulk electrochemical experiments were conducted using a two-electrode system in a 40 mL Pyrex beaker fitted with a Teflon cap. The Teflon cap had holes for the introduction of electrodes and thermometer. During the experiment the temperature was continuously monitored. The area of the titanium anode and cathode that was in contact with electrolyte had a dimension of 12 × 15 mm. The two electrodes were immersed into the electrolyte that was maintained at a constant temperature by placing it on a Corning thermostat. The precision of the Corning thermostat was determined to be ±2 °C**.** Once the temperature was constant for 30 min, a potential was applied across it using Princeton applied research model A273. Experiments were carried out for 2–4 h at three different temperatures of 140, 150 and 160 °C. After each experiment, the electrolyte was stored in a glass bottle. The material deposited at the cathode was thoroughly washed with acetone and water. For XRD analysis, samples were ground and mounted on a silica glass, which was then mounted into the Philips PW 3038 diffractometer. The scan rate for the XRD measurement was kept constant at 0.02 s^{-1} and the sample was scanned from 20 to 90°.

For Chronoamperometric studies, a three-electrode cell was used. The electrochemical studies was investigated on a titanium-working electrode. The reference and counter electrodes were Ag quasi reference electrode and platinum, respectively. The contact area of the working electrode with the electrolyte was 0.025 cm^2. FTIR analysis was carried out using Perkin Elmer FTIR-ATR instrument. For FTIR analysis one drop of the sample was placed on the diamond base and the absorption data was collected on a computer-based software.

3 Results

Figure 1 demonstrates the current versus time plot during the electrolysis of $NiCl_2$-1-ethyl-3-methylimidazolium chloride ($NiCl_2$-EmimCl) on applying 3.0 V at different temperatures. It is observed that there is almost a linear rise in current for initial 0.05 and 0.24 h for temperatures of 140 and 150 °C, respectively. After the initial rise, the current steadily drops to 34 mA at 140 °C whereas at 150 °C there is a plateau region for the next 0.25 h and then the current drops to 70 mA. On performing electrolysis at 160 °C, the current continuously rises for 1.4 h after which it plateaus. It was observed on continuing the electrolysis for greater than 2 h that the current steadily decreases.

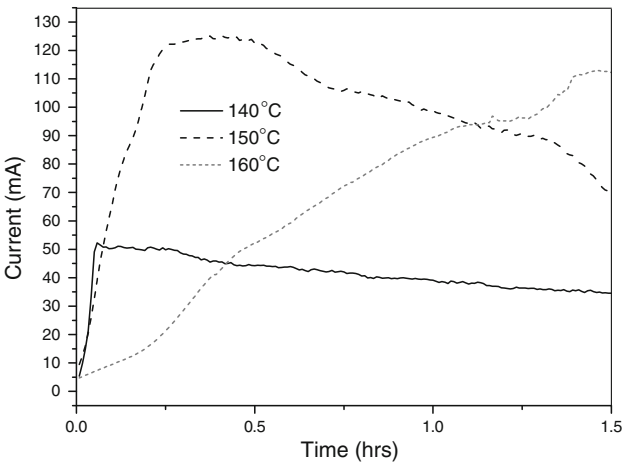

Fig. 1 A plot of current time diagram during electrolysis of $NiCl_2$-EmimCl at different temperature

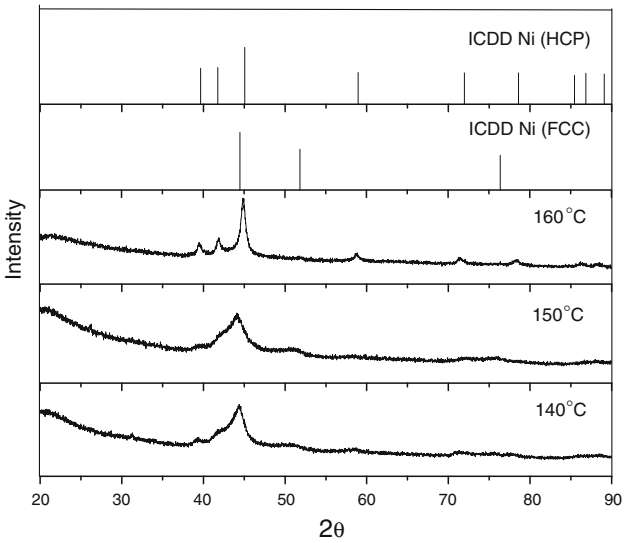

Fig. 2 Comparison of XRD data of the electrodeposited material obtained at different electrolysis temperature

The diffraction patterns of electrodeposited nickel obtained at different temperatures are compared in Fig. 2. It is evident from the XRD patterns that on performing electrolysis at 140 and 150 °C, nickel forms FCC phase whereas HCP phase is formed at 160 °C. The microstructure of the electrodeposited nickel obtained at 140 and 160 °C is compared in Fig. 3a and b. Both microstructures show nodular deposit. The EDX spectra of both the deposits confirm the formation of nickel. A chlorine peak is observed in the EDX spectra in Fig. 3b and could be due to small amount of ionic liquid present in the deposited HCP nickel sample. Although XRD pattern showed the formation of FCC and HCP nickel phase at the two temperatures, the microstructure does not show any radical difference.

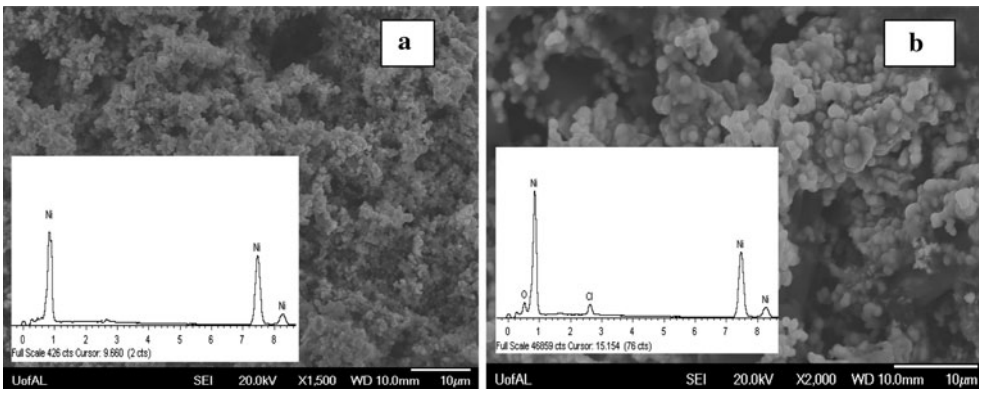

Fig. 3 **a** Microstructure of the electrodeposited nickel (FCC phase) at 140 °C. *Inset* shows the EDX spectra. **b** Electrodeposited nickel (HCP phase) at 160 °C. *Inset* shows the EDX spectra confirming nickel

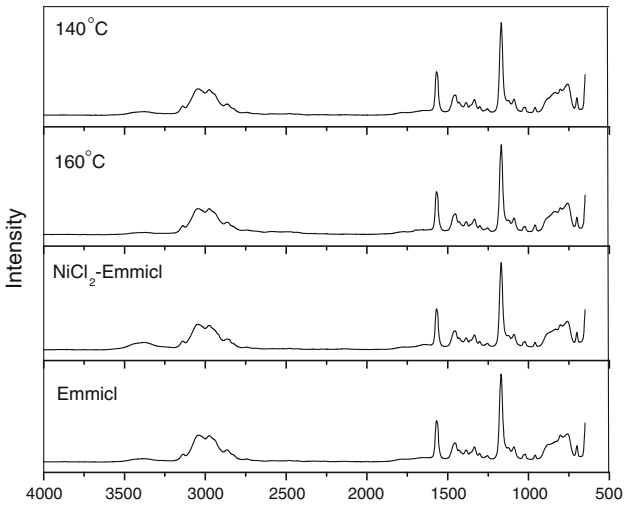

Fig. 4 Comparison of FTIR plots of EmimCl, EmimCl-$NiCl_2$, and electrolyte after performing electrolysis at 140 and 160 °C

The FTIR of the electrolyte at various stages of the electrolysis process are compared in Fig. 4. The plots show peaks of aromatic, aliphatic and ring structure groups. In pure EmimCl, the aromatic C–H bond occurs at 3043 and aliphatic C–H bond at 2973 cm^{-1}. The peak at 2864 cm^{-1} corresponds to the N–H bond [9]. Ring stretching symmetries are observed at 1566, 1453, 1334 and 1173 cm^{-1}. The methyl group C–H bond occurs at 1383 and 1334 cm^{-1}. The C–H ring structure in-plane bending is observed at 1092 cm^{-1} and an N–H bond at 957 cm^{-1}. A broad outer plane asymmetric ring bending is present at 758 cm^{-1}.

On addition of $NiCl_2$ in EmimCl, few changes take place in the FTIR peaks. There is a decrease in the intensity at 3049 cm^{-1} which is the Cl^- interaction band [10]. Although from the graph the decrease in the intensity is not clear, numerical values show a decrease by 15%. This might be due to the formation of $NiCl_4^{2-}$ phase from which nickel can be electrodeposited [11]. Furthermore, we find growth of small peak at 3386 cm^{-1} which is the OH stretching and indicates the presence of moisture in $NiCl_2$. No OH stretching peak was observed in EmimCl. Using thermogravimetric analysis (TGA) the water content in $NiCl_2$ was found to be 2 wt%. After performing electrolysis at 160 °C, no OH stretching is observed whereas there is a small OH stretching at 140 °C. Thus, FTIR studies indicate the role of moisture in producing different nickel structure.

4 Discussion

During electrolysis at 140 and 150 °C, the initial current rise was linear. This may be due to Ni deposition on the Ti electrode whereby there is a decrease in resistance. On continuation of electrolysis, the decrease in current may be related to decrease in the concentration of $NiCl_2$ in the solution. At higher electrolysis temperature, the conductivity of the electrolyte increases which results in increased current flow across the electrodes. Therefore the current flow at 150 °C is higher compared to that at 140 °C. In comparison, the current time plot at 160 °C is different. This might be due to a secondary reaction at 160 °C. The presence of secondary reaction is confirmed by the fact that FCC structure was obtained at 140 and 150 °C whereas HCP structure was obtained at 160 °C as seen in the diffraction pattern in Fig. 2.

It was confirmed from TGA analysis that $NiCl_2$ contained 2 wt% moisture. Additionally, FTIR of the electrolyte after the electrolysis at 140 °C showed OH stretching whereas no OH stretching was observed at 160 °C. Therefore, we could say that the formation of HCP nickel occurs due to the presence of hydrogen, which is formed by the electrolysis of water.

DSC analysis showed that HCP Ni transformed to FCC Ni at 422.6 °C [12]. Hydrogen analysis of FCC and HCP Ni carried out by Midwest Microlab confirmed that HCP Ni had 1.2% hydrogen and FCC Ni had no hydrogen.

To confirm that H_2O present in $NiCl_2$ is the source of hydrogen in Ni, the moisture was removed by heat treating $NiCl_2$ at 800 °C in argon atmosphere for 2 h. The salt was

then cooled to room temperature in argon atmosphere and quickly transferred to the argon filled glove box. $NiCl_2$ was then and dissolved into the ionic liquid. On performing electrolysis at 160 °C, FCC nickel phase was produced which confirms that moisture was responsible for the formation of HCP phase. At this point we could say that the secondary reaction and the steady increase in current at 160 °C observed in Fig. 1 could be due to the contribution of H^+ ions diffusing in the electrolyte.

To evaluate the reaction kinetics of the electrodeposition process, chronoamperometric technique was adopted. The current–time plot is shown in Fig. 5. From the Chronoamperometric curve, an initial rise in current is noted which is due to the formation and growth of nickel nuclei. On reaching a current maximum i_m at time t_m, the curve decays. As the potential is stepped up, i_m increases whereas the maximum time t_m shortens.

For a metal deposition process, a 3-D nucleation growth model is usually reported [13, 14]. However, the nucleation mechanisms are of two different types. In one case, instantaneous nucleation occurs wherein the metal is deposited uniformly over the entire surface and then grows at a constant rate which depends on the applied potential. The second case is the progressive nucleation of the electrodeposited metals wherein the nuclei grow at different rates and depend on the time of their deposition [15, 16].

The current transients for the electrodeposition of nickel from $NiCl_2$-EmimCl were analyzed using the methodology developed by Hills and Scharifker [16]. They developed models for both instantaneous nucleation and progressive nucleation mechanism as represented by Eqs. 1 and 2, respectively.

$$\left(\frac{i}{i_m}\right)^2 = 1.9542\left(\frac{t_m}{t}\right)\left(1-\exp\left[-1.2564\left(\frac{t}{t_m}\right)\right]\right)^2 \quad (1)$$

$$\left(\frac{i}{i_m}\right)^2 = 1.2254\left(\frac{t_m}{t}\right)\left(1-\exp\left[-2.3367\left(\frac{t}{t_m}\right)^2\right]\right)^2 \quad (2)$$

In Eqs. 1 and 2, 'i' represents the current density at any time 't', 'i_m' is maximum current density (A/cm^2) at time 't_m'. Plots of $(i/i_m)^2$ vs t/t_m for $NiCl_4^{2-}$ reduction in $NiCl_2$-EmimCl along with the theoretical predictions according to Eqs. 1 and 2 are shown in Fig. 6. It is evident from Fig. 6 that the experimental data provides a much better fit for the progressive nucleation mechanism.

To evaluate the diffusion coefficient of $NiCl_4^{2-}$, we could use the Cottrell equation. Neglecting the growth of the electrode area, the diffusion coefficient calculated by this method gives a value of 1.5×10^{-5} cm^2 s^{-1}. When the deposition proceeds by progressive nucleation mechanism, Eq. 3 proposed by Hill and Scharifker [14] can be used to calculate diffusivity of $NiCl_4^{2-}$ species.

$$i_m^2 t_m = 0.2598(nFC_{bulk})^2 D \quad (3)$$

In Eq. 3, n (charge of the ion) is 2, F is the faraday constant and D is the diffusion coefficient. By substituting the values in Eq. 3, the diffusion coefficient D was found to be 1.1×10^{-5} cm^2 s^{-1}. This value is comparable to that obtained by Cottrell equation. Deng et al. [17] obtained a diffusion coefficient in the range of 10^{-6} cm^2 s^{-1} for the electrodeposition of nickel from ionic liquid at room temperature. As the experiment performed in the present case was at 150 °C the diffusion coefficient value increased to 10^{-5} cm^2 s^{-1}.

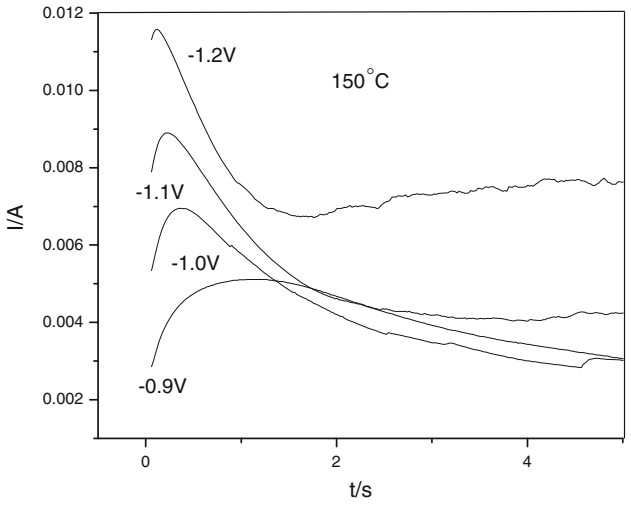

Fig. 5 Chronoamperometric current versus time responses obtained for the reduction of 5.4 mM $NiCl_2$-EmimCl at 150 °C when the potential is stepped from −0.9 to −1.2 V

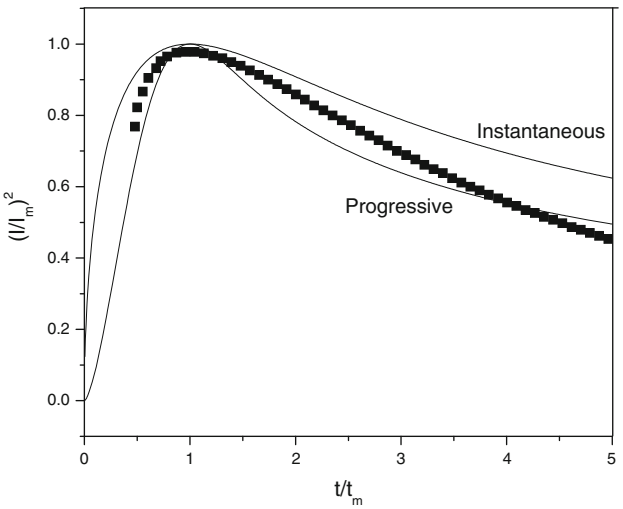

Fig. 6 Comparison of Plot of $(i/i_m)^2$ vs t/t_m obtained from Chronoamperometric experiments for reduction of 5.4 mM of $NiCl_2$-EmimCl at 150 °C with the theoretical plots derived for instantaneous and progressive nucleation

5 Conclusions

1. Electrolysis at 160 °C produces hydrogen by the decomposition of water present in $NiCl_2$ and results in deposition of HCP Ni. Electrolysis at lower temperature does not decompose water and produces FCC Ni.
2. HCP nickel contains 1.2 wt% hydrogen. The transformation temperature of HCP nickel to FCC nickel occurred at 462 °C releasing hydrogen in the process.
3. The electrodeposition process was governed by progressive nucleation mechanism. The diffusion coefficient for the electrodeposition of Ni from NiC_{l2}-EmimCl was found to be around 1.1×10^{-5} $cm^2\ s^{-1}$.

Acknowledgments The authors gratefully acknowledge the ACI-PCO, The University of Alabama, Dr R Reddy for providing the laboratory facilities. The authors would also like to thank Dr Scott Spear for his useful suggestions and help with FTIR.

References

1. Hemenger P, Weik H (1965) Acta Crystallogr A 19(4):690–691
2. Tuaillon J et al (1997) Philos Mag Phys Condens Matter 76(3):493–507
3. Wayman ML, Weatherly GC (1990) Binary alloy phase diagrams. ASM International, Ohio
4. Shizuku Y, Yamamoto S, Fukai Y (2002) J Alloys Compd 336(1–2):159–162
5. Hidayat T et al (2009) Metall Mater Trans B Process Metall Mater Process Sci 40(1):1–16
6. Carturan G et al (1988) Mater Lett 7(1–2):47–50
7. Mi Y et al (2005) Mater Chem Phys 89:359–361
8. Yang L (1950) J Electrochem Soc 97(9):241–244
9. Tait S, Osteryoung RA (1984) Inorg Chem 23(25):4352–4360
10. Dieter KM et al (1988) J Am Chem Soc 110(9):2722–2726
11. Gou SP, Sun IW (2008) Electrochim Acta 53(5):2538–2544
12. Lahiri A, Tadisina Z (2010) Mater Chem Phys. doi:10.1016/j.matchemphys.2010.07.019
13. Ziegler JC, Wielgosz RI, Kolb DM (1999) Electrochim Acta 45:827–833
14. Bhatt AI, Bond AM, Zhang J (2007) J Solid State Electrochem 11:1593
15. Bulhoes LOS, Mascaro LH (2004) J Solid State Electrochem 8(4):238–243
16. Scharifker B, Hills G (1983) Electrochim Acta 28:879
17. Deng MJ et al (2008) Electrochim Acta 53(19):5812–5818